# MULTIDISCIPLINARY DESIGN OPTIMIZATION FOR A TAILLESS UNMANNED AERIAL VEHICLE WITH ELECTRICAL PROPULSION USING THE WEISSINGER L-METHOD AS A COMPUTATIONAL TOOL TO OBTAIN THE WING AERODYNAMIC CHARACTERISTICS

**Alejandro Arturo Rios Cruz**
aarios@ita.br
**Saulo Barbosa Oliveira**
neosoyo@gmail.com
**Paulo Afonso de Oliveira Soviero**
soviero@ita.br
**Luiz Carlos Sandoval Góes**
goes@ita.br
Instituto Tecnológico de Aeronáutica, Praça Mal. do ar Eduardo Gomes, 50, Vila das Acácias - São José dos Campos - SP - Brazil

***Abstract.*** *A project of multidisciplinary design optimization demands a consistent model of all the disciplines involved in it. As a consequence, most of the computational consumption is employed in the execution of all these disciplines. Currently there is only a few multidisciplinary design optimization methods for tailless aircrafts. This configuration may represents advantages if compared with other configurations for several aircraft tasks, as UAV's (Unmanned Aerial Vehicle) market, because of the gain in aerodynamic efficiency (reduction of energy consumption), simplicity of construction and increasing of the internal space for device's arrangement.*
*This paper presents the development of a MDO (Multidisciplinary Design Optimization) for the project of a tailless UAV configuration UAV. The main objective of the optimization is to maximize endurance and minimize empty weight having as principal input variables the wing's geometrical parameters. For that the mass of the electronic components in each subject was considered to calculate aerodynamics and performance.*
*One of the most important MDO's innovation presented on this paper is the use of the Weissinger method as a computational tool. The purpose of using it is it's capability to calculate wing's aerodynamics characteristics shifting aspect ratio, taper ratio, wing swept (positive and negative) and geometrical twist, offering a better trade-off between accuracy and computational effort, improving considerably the time of execution, if compared with other commonly used methods for instance the vortex lattice method. For the endurance evaluation it was considered the modified performance equations for electric motor. The choice of this kind of propulsive system is based on the current tendency of using cleaner and renewal energies in aeronautical applications.*

***Keywords:*** *MDO, Tailless Aircraft, Electric Propulsion,Weissinge L-Method,UAV*

## 1. Introduction

Unmanned Aerial Vehicles (UAV's) have become one of the most popular aeronautical technologies in the last years. The usage of this kind of technology is being increased day by day. It has being opening different potential markets and challenging the UAV's company's to improve quality of the air-frames and their embedded technology's. Accordingly with its needs, more sophisticated aircraft design tools are being applied in order to obtain aircraft's with better mission performance.

Nowadays most of the aviation companies use Multidisciplinary Design Optimization to improve their design in more than one area. As result they obtain air-frames that are optimized for a particular predefined task. This kind of tools requires analysis of as many individuals as possible: the angular key to improve the design models became the implementation of methods to calculate the black boxes with minimal computational effort.

## 2. Weissinger L-Method Description

The selected tool to perform the calculation of the aerodynamic parameters in the MDO was the Weissinger L-Method. Presented by Weissinger (1947) it consists on an extension of the lifting line developed by Prandtl, with the difference that the first one allows the calculation of wings with high values of sweep angle and aspect ratio. Weissinger L-Method is used instead of others because of it's vantages to perform the same calculations of other line or surface methods - such as VLM, Panel Method or CFD - with a very low computational effort. To minimize it's disadvantages referring to the calculation of profile drag (lifting line theories only calculate induced drag) a correction is performed implementing strip theory.

Extended lifting line's physics relates the downwash to an specified span station on the wing to the sum of the downwash velocity induced by the bound vortex (vortex line attached to the quarter chord line) and free vortex (with infinity extension). The wing discretization as specified by the method is represented in Figure 1.

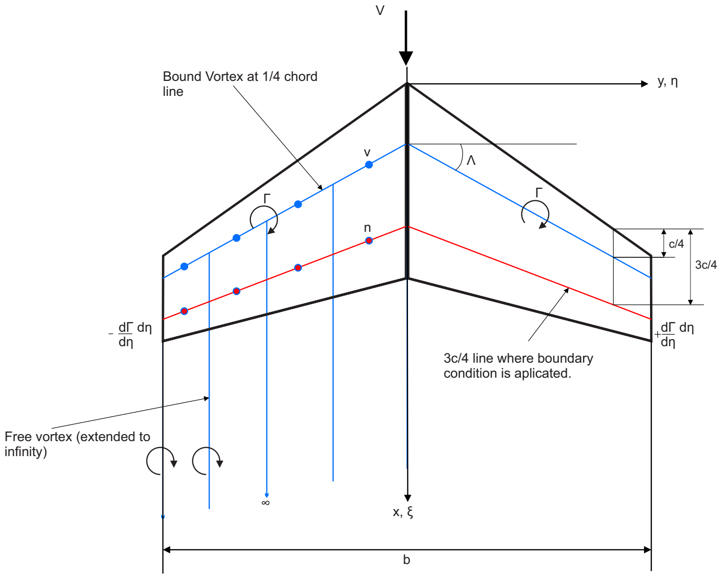


Figure 1. Weissinger L-Method wing model.

The boundary condition applied to determine the value of circulation $\Gamma$, named as "kinematic condition" or "no flow through surface condition", stipulates that the airflow should be tangent to the surface at the three quarter chord line of the wing. As it can be seen in Figure 1, each control point is defined at the intersection of the horseshoe vortex centre-line at the wing three quarter chord line.

The useof the Biot-Savart law in order to obtain the downwash generated by the bound and free vortex resulted into a integro-diferential equation for the total downwash.

$$
\begin{aligned}
w(x,y) = {} & \frac{2}{4\pi}\int_{-b/2}^{b/2}\frac{\Gamma'(\bar{y})d\bar{y}}{y-\bar{y}} \\
& + \frac{1}{4\pi}\int_{-b/2}^{0}\left[\frac{\sqrt{(x+\bar{y}\tan(\Lambda))^2+(y-\bar{y})^2}}{(x+y\tan(\Lambda))(y-\bar{y})} - \frac{1}{y-\bar{y}}\frac{2\tan(\Lambda)\sqrt{x^2+y^2}}{x^2-y^2\tan^2(\Lambda)}\right]\Gamma'(\bar{y})d\bar{y} \\
& + \frac{1}{4\pi}\int_{0}^{b/2}\left[\frac{\sqrt{(x-\bar{y}\tan(\Lambda))^2+(y-\bar{y})^2}}{(x-y\tan(\Lambda))(y-\bar{y})} - \frac{1}{y-\bar{y}}\right]\Gamma'(\bar{y})d\bar{y}
\end{aligned} \tag{1}
$$

$w$ is the induced velocity at the coordinates $x$, $y$, $\Gamma$ is the value of circulation and $\Lambda$ is the geometric swept angle of the quarter chord line.

Using numerical tools, like the trapezoidal integration and the Gaussian quadrature formula Multhopp (1955), Weissinger solved the downwash integral presented in Equation 1. After applying algebra and simplifications the downwash angle equation can allow solution by simultaneous equations as shown in Equation 2.

$$
\left(\frac{w}{U}\right) = (2b_{vv} + \frac{b}{c_v})G_n - \sum_{i=1}^{n}{}' (2b_{vn} - \frac{b}{c_v}g_{vn})G_n \tag{2}
$$

$(\frac{w}{U})$ is the downwash angle, $b_{vv}$ and $b_{vn}$ are the mathematical series coefficients, $G_n$ is the dimensionless circulation $(\frac{\Gamma}{bU})$ and $\frac{b}{c_v}$ is the ratio between the wing span and the local chord.

Equation 2 can be simplified as shown in Equation 3

$$
\alpha_v = \sum_{n=1}^{\frac{m+1}{2}} a_{vn}G_n \tag{3}
$$

$\alpha_v$ is the angle of attack at each station and $a_{vn}$ represent the influence coefficients that depends only on the wing geometry.

As described by Weissinger, the method is applied for wings which are represented by a flat plate. Corrections may be done in order to enable the introduction of other wing sections. To solve this issue, the left side of the Equation 3 should be substituted by the following expression:

$$\frac{C_{l_{\alpha v}}}{2\pi}\left[\alpha_v - \alpha_{L=0v}\right] \tag{4}$$

$C_{l_{\alpha v}}$ and $\alpha_{L=0v}$ are the slope of the lift curve and the angle of attack for zero lift of the arbitrary section correspondingly. Such parameters are calculated using a subroutine that runs the 2D panel method (Xfoil).

Solving the equation 3 for a determined number of control points, the result was a system of m unknowns with m equations as shown by 2.

$$\begin{bmatrix} \frac{C_{l_{\alpha v}}}{2\pi}\left[\alpha_v - \alpha_{L=0v}\right] \\ \frac{C_{l_{\alpha v}}}{2\pi}\left[\alpha_v - \alpha_{L=0v}\right] \\ \vdots \\ \frac{C_{l_{\alpha \frac{m+1}{2}}}}{2\pi}\left[\alpha_{\frac{m+1}{2}} - \alpha_{L=0\frac{m+1}{2}}\right] \end{bmatrix} = \begin{bmatrix} a_{1,1} & a_{1,2} & \cdots & a_{1,\frac{m+1}{2}} \\ a_{2,1} & a_{2,2} & \cdots & a_{2,\frac{m+1}{2}} \\ \vdots & \vdots & \ddots & \vdots \\ a_{\frac{m+1}{2},1} & a_{\frac{m+1}{2},2} & \cdots & a_{\frac{m+1}{2},\frac{m+1}{2}} \end{bmatrix} \begin{bmatrix} G_1 \\ G_2 \\ \vdots \\ G_{\frac{m+1}{2}} \end{bmatrix}$$

The result of the equations system is the circulation at each span station of the wing, allowing the calculation of other aerodynamic parameters from the circulation $\Gamma$, such as the lift, drag and moment coefficients in equation 5.

$$C_L = \frac{L}{qS}, \quad C_{Di} = \frac{Di}{qS}, \quad C_M = \frac{Mb}{qS^2} \tag{5}$$

$q$ is the dynamic pressure and $S$ the wing surface.

In order to insert the profile drag contribution to the total drag's sum, an approximation using strip theory was done. This theory sub-divides the wing into small spanwise strips where the bi-dimensional aerodynamic coefficients are calculated. It's not necessary to apply corrections into the strip theory because the Weissinger L-Method already considers the three-dimensional effects of the wing. Applying the weighted average of the profile drag generated by each strip it was found an approximated value of the total profile drag of the wing.

Finally, the evaluation of the wing stall angle was executed using the critical section method. This calculation uses the spanwise lift distribution obtained by Weissinger L-Method and the bidimensional $cl_{max}$ calculated by Xfoil at several wing stations. The value of the wing angle of attack was iterated between a predefined interval; it stops occur when the lift distribution curve is tangent to the line of the 2D maximum lift, as represented in figure 2

## 3. Airfoil selection

The selection of a proper wing section for tailless aircraft's is a complex task that requires knowledge of the behavior presented by the change of different shape parameters.

Auto-stabilizing wing sections (or reflex wing sections) demands predefined behavior to ensure performance and stability. These requirements are based on the kind of tailles wing that is being designed. The presented MDO evaluate two kinds of tailless configuration aircraft's, Plank and Swept Back. In the selection of the proper airfoil, which is a constant input on the MDO, the follow characteristics were considered:

- Moment coefficient $Cm \approx 0$ or positive.
- Lift coefficient as higher as possible.
- Thickness to chord ratio that provides sufficient space to place electronics.

The first two characteristics involve a compromise solution that was evaluated in order to reach a proper airfoil. The correct combination between amount of camber, reflex and maximum camber position yields to an airfoil with low moment coefficient that maintain a high lift coefficient. Special care was taken to velocity distributions to estimate flow separation (stall characteristics), once reflex airfoils are sensitive at low Reynolds numbers.

As specified in reference Hepperle (2005), the best compromise for light tailless airplanes seems to be a moderately reflex camber line, combined with the maximum camber shifted towards the leading edge and a rather blunt nose. Associating a smooth velocity distribution, a soft stalling character can be achieved.

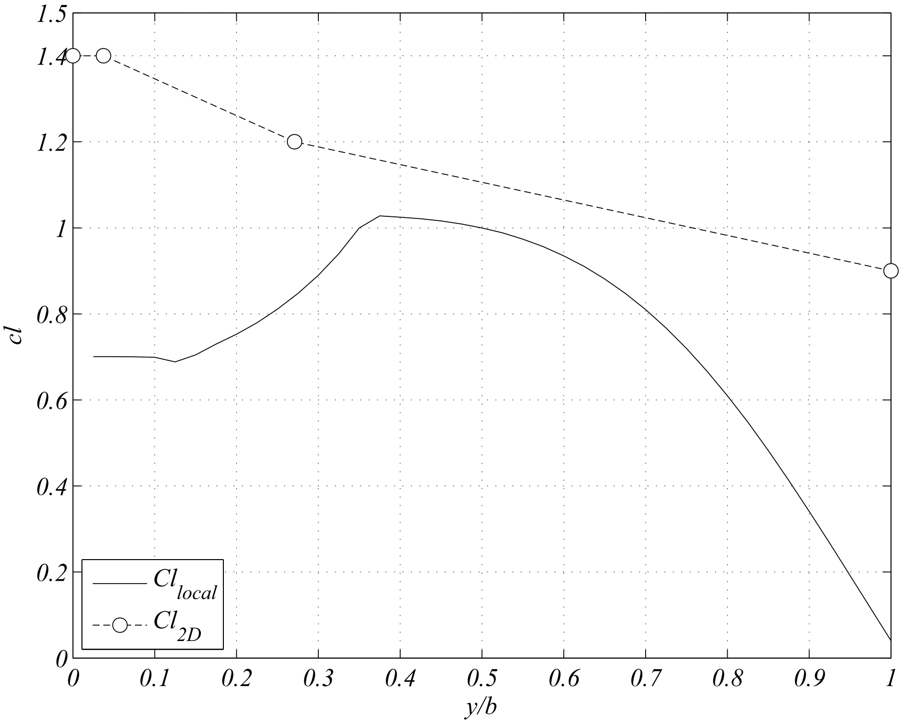

Figure 2. Critical Section Method.

Concerning the stall characteristics, the airfoil plays an important role, but only in conjunction with the spanwise lift distribution, which is a result of the wing plan-form and the spanwise twist distribution. Swept and tapered wings tend to have a higher loading near the wing tip, which causes the tip to stall first if no additional twist is used.

Considering this information, it was executed a systematical study of existing reflex airfoils, the combinations between them, and its modifications to achieve the intended characteristics. The study results in a new airfoil that has been already analyzed and tested by an AeroDesign's competition team demonstrating agreement with the theoretical analysis. Figure 3 shows the principal characteristics of the "Alesky" airfoil.

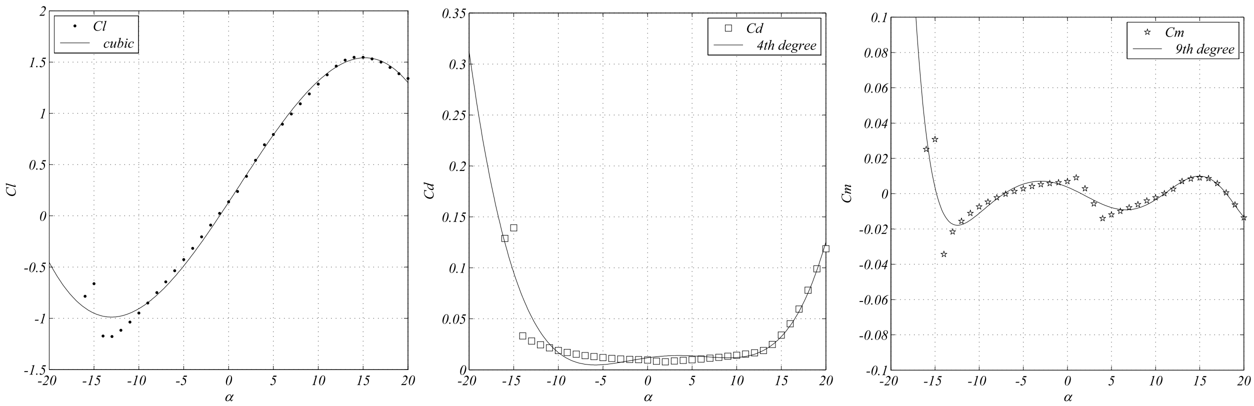

Figure 3. Wing section aerodynamic coefficients Cl, Cd and Cm for a $Re = 5e5$

## 4. MDO objectives

The fundamental objective of this MDO was to produce a very competitive market-ready micro-class UAV system. To determine the essential design parameters for the optimization, some conceptual considerations were raised up:

1. Minimal control surfaces;
2. Hand-launched possibility;
3. Basic electronic setup for autonomous flight / computer vision missions;
4. High endurance;

5. Portability.

A initial design was developed (figure 4), based primarily on the third consideration.

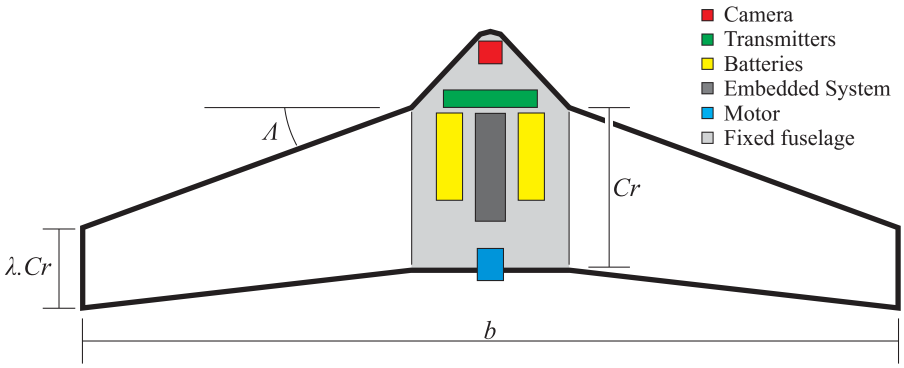


Figure 4. Initial design.

Four fundamentals design parameters determine the geometry inputs to construct the air-frame. These parameters are the wingspan $b$, sweep angle $\Lambda$, taper ratio $\lambda$ and the twist angle $\epsilon$. Thus, the minimum flight velocity $V_{min}$ is an essential performance parameter to be restricted too.

The internal fuselage volume was modeled in order to ensure the minimal space to place an specific setup that contains the following items:

- One 900Mhz and one 2.4Ghz radio transmitters;
- 2.4 Ghz Receiver for RPAS;
- Two 6s Lipo batteries with 8500mAh each;
- One Autopilot;
- One Linux mini computer;
- One HD camera;
- EPP material construction;
- Power management and electric motor for propulsion.

Latero-directional stability augmentation is performed by a winglet wing tip which was designed based on Simons (1994). This solution was selected in order to avoid the need to another kind of yaw control (like drag-rudders). The effect of this winglet wasn't considered in the aerodynamic calculation because the program is already developed and the validation of that kind of surface is in progress. Thus, the effect of the winglet was only weighted in the mass analysis. As specified before, the air-frame must carry on a fixed payload with maximum endurance. The empty weight (consequently the MTOW) was minimized and the endurance was maximized.

## 5. Design Parameters Intervals

Based on experience and common sense the design parameters intervals were defined as follow. The wingspan $b$ was limited to 2 meters. This upper limit ensures high values of wing area at the same time that allows wing sectioning to minimize required transportation volume space for a portable version of the aircraft. The minimum wingspan adopted was 0.7 meter, because low wingspan affects the aerodynamic efficiency and can result in aggressive maneuver behavior, specialty on latero-directional movement for flying wings designs.

The sweep angle $\Lambda$ interval was adopted to be between 0 to 30 degrees. The main reason of this decision is to ensure a good static margin $SM$ value, which, based on Nickel and Wohlfahrt (1990), have to be between 3% to 7% for flying wings.

The taper ratio $\lambda$ varies between 0.3 to 1. It guarantees a minimum tip chord for winglet construction at the same time that provides the possibility to obtain configurations with better aerodynamic efficiency.

At last, an interval of twist angle $\epsilon$ at the tip chord of the wing, with the intention to adjust the wing stall start position $y_{stall}$ of sweep wings, was introduced as a parameter. The intended behavior of this entry is illustrated in Figure 5. The stall cannot start over a control surface, the aircraft must have control authority to recover from stall. Thus the $\epsilon$ varies between -4 to 0 degrees. The Table 1 summarize the design parameters interval.

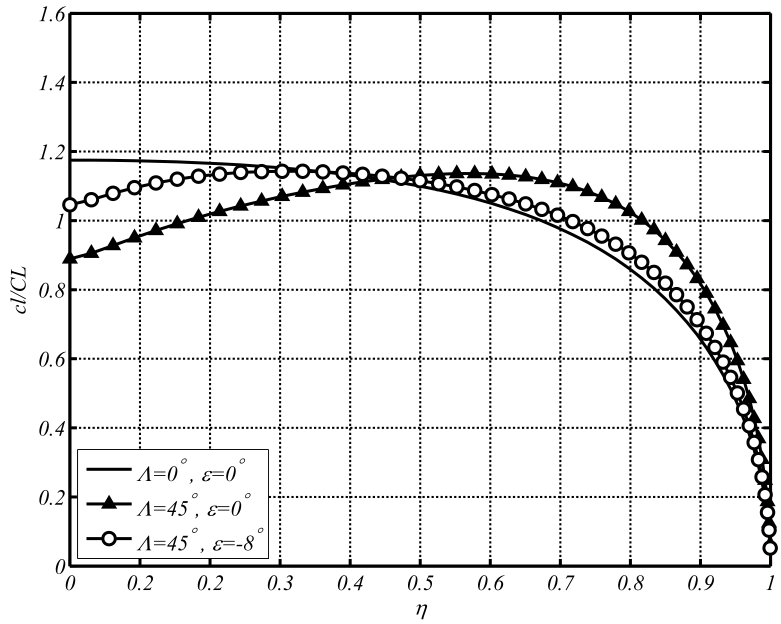


Figure 5. Twist justification.

| Minimum | Variable | Maximum |
|---|---|---|
| $0.7[m]$ | $b$ | $2[m]$ |
| $0°$ | $\Lambda$ | $30°$ |
| $0.3$ | $\lambda$ | $1$ |
| $-4°$ | $\epsilon$ | $0°$ |

Table 1. Design Parameters interval.

## 6. Restrictions

From the first to fourth conceptual considerations, the $V_{min}$ was adopted to be between 9 to 12 $m/s$, mainly based on information of hand-launched aircraft performance from SAE Brazil AeroDesign micro class competition. Furthermore, higher velocities implies on higher power consumption, degrading the endurance. Slower flights also contribute to better image capturing, but *too low* velocities affect negatively the control performance.

Table 2 summarize this restrictions.

| Minimum | Variable | Maximum |
|---|---|---|
| - | $y_{stall}$ | $50\%$ of $b$ |
| $3\%$ | $SM$ | $7\%$ |
| $9[m/s]$ | $V_{min}$ | $12[m/s]$ |

Table 2. Restrictions.

## 7. Empty weight and C.G. prediction

The open-source parametric aircraft modeler, OpenVSP (created by NASA), was used to determine the weight, inertia's and C.G. of aircraft. All the electronic components were modeled in this program and a relative density was calculated and set to achieve the approximated real weight (figure 6).

The OpenVSP allows design files, linking geometry variables to automatic sizing and batch command, allowing the interaction with Matlab via a function `dos()` and specific script for OpenVSP.

## 8. Propulsion and performance method

Based on market availability, an engine-propeller setup focusing on efficiency prior performance was chosen. Using the base design weight shown in figure 4 and respecting the $T/W$ relation of 0.4 (Torenbeek (2013)) to minimize energy consumption, the static traction was determined.

By Traub (2011), the maximum endurance time can be estimated using the equation:

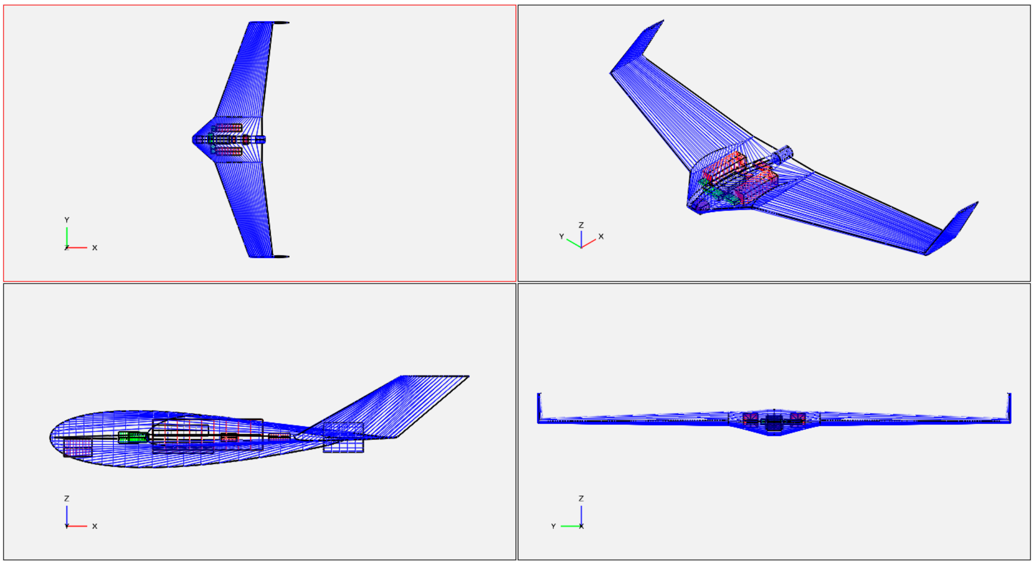


Figure 6. Base design modeled on OpenVSP.

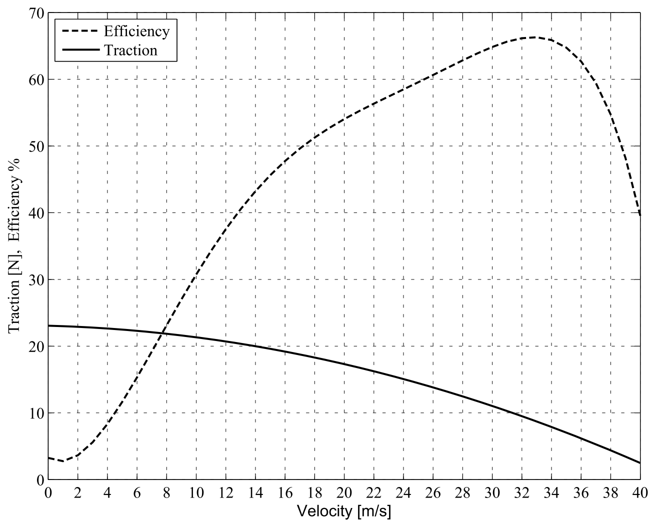


Figure 7. Engine model.

$$E_{max} = Rt^{1-n} \left[ \frac{\eta_t V \times C}{\left( \frac{2}{\sqrt{\rho S_{ref}}} \right) C_{D_0}^{1/4} \left( 2W\sqrt{k/3} \right)^{3/2}} \right]^n [h] \tag{6}$$

$Rt$ is the discharge time over the battery's capacity (typically 1 hour), $\eta_t$ is the propulsion efficiency shown in figure 7, $V$ is the battery nominal voltage and $C$ it's capacity in ampere hour. The discharge parameter $n$ varies from type, age, discharge rate and temperature of battery. For the presented study, it was considered the worst scenario relative to the value of $n = 1.4$. The values of $W$, $k$ and $C_{D_0}$ were determined from the air-frame geometry using OpenVSP and the aerodynamic tools specified before.

## 9. MDO configuration

The Figure 8 illustrate the MDO process developed on Matlab®. It was used MOGA-II optimization algorithm with penalizing objectives under modeFRONTIER® environment. The initial population size was 100 individuals, using SOBOL algorithm.

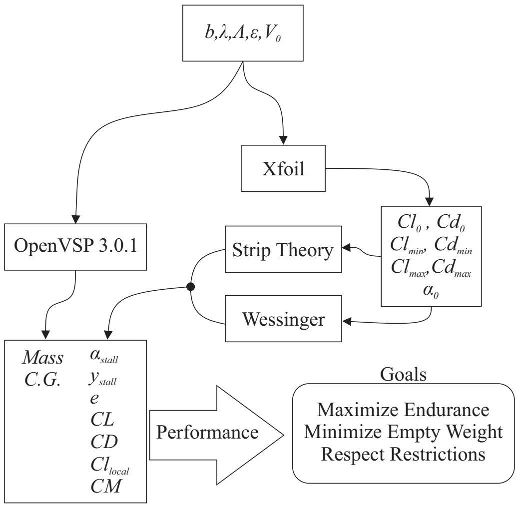


Figure 8. MDO fluxogram.

## 10. Results

The workstation is equipped with AMD® Phenom III 1100T processor, 16GB of RAM and SSD hard-drive. The Table 3 summarize the average time consumption for each main task of the MDO flowchart, comparing the Wessinger method developed on Matlab with AVL (Athena Vortex Lattice).

| Process | Method | Time |
|---|---|---|
| Geometry construction and mass prediction | Matlab+OpenVSP | $4.1264 \pm 0.00234[s]$ |
| Aerodynamic | Xfoil+Wessinger | $9.942 \pm 0.0134[s]$ |
| Aerodynamic | Xfoil+AVL | $43.318 \pm 0.0761[s]$ |
| Performance and results | Matlab | $0.0024 \pm 0.0001[s]$ |
| modeFRONTIER process | - | $6.592 \pm 0.0023[s]$ |

Table 3. Speed performance for each MDO process.

Figure 9 shows the deviation between the two aerodynamic methods, with a peak value of 0.93%.

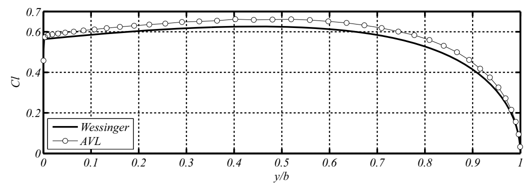


Figure 9. Wessinger and AVL $Cl$ distribution for a generic flying wing.

The Wessinger method for aerodynamic process was up to 77% faster than AVL. The decrease of total time consumption was 38.2%. After 123 generations, a total of 12300 individuals was calculated in ≈3 days of computational time.

| Variable | Median | Standard deviation |
|---|---|---|
| $SM$ | 5.18 | $\pm\ 0.836\ \%$ |
| $y_{stall}$ | 33.27 | $\pm\ 5.0679\ \%$ |
| $V_{min}$ | 12 | $-\ 0.63\ m/s$ |

Table 4. Statistical data of feasible individuals.

The dispersion of unfeasible individuals on Figure 10 indicates that the mutation probability of 35% emulates the appearing of *species* on the system's evolutionary context. The pareto front shown in figure 11 is consistent and composed by 34 individuals.

By figure 12, five species can be identified. The dot over a group of pareto individuals indicates the median point for static margin and $y_{stall}$; the dotted square indicates the standard deviations. This information indicates where the *strongest genetic characteristics* occurs at the pareto group, helping to decide which pareto individual will be post-processed.

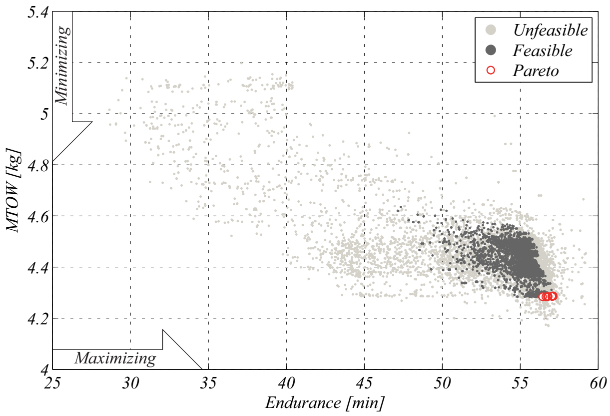


Figure 10. Objectives history chart.

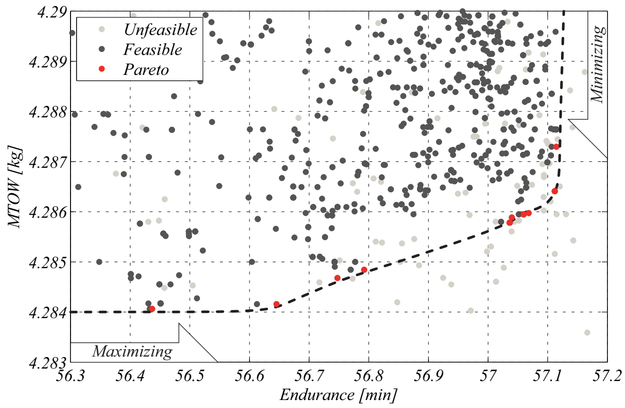


Figure 11. Pareto front.

The aircraft shown in figure 13 is derived from pareto group closer to median point. It can fly up to 57 minutes with $MTOW$ of $4.203[kg]$ and $b < 1[m]$.

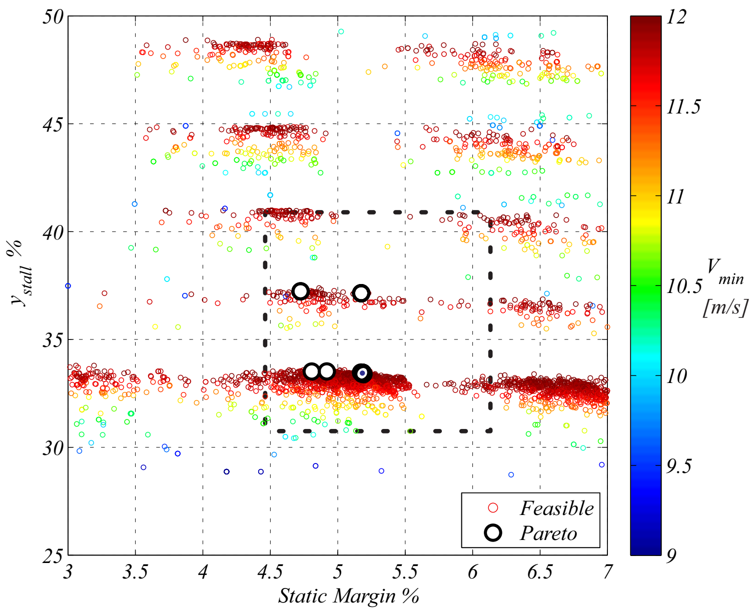


Figure 12. Restrictions on feasible individuals.

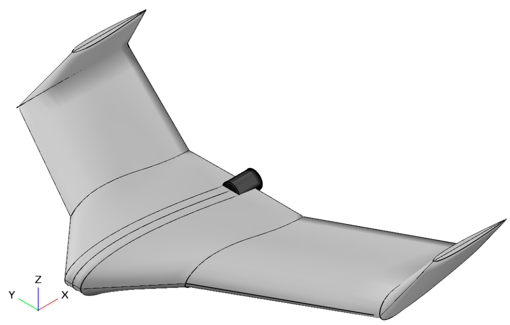

Figure 13. Optimized individual.

There are many other ways to select an optimized individual in pareto group and it mostly depends on the knowledge about the system. A practical way to do it is to execute some post-processing jobs over the pareto group that the black boxes don't execute. For aircrafts, the stability and structural design constraints are more often utilized to exclude individuals from pareto Charles A. Mader (2013).

## 11. Conclusions

A methodology for the MDO of tailless aircraft for the micro UAV class is presented. The developed tools are alternatives to perform the black box calculations on aircraft MDO, improving considerably the individuals time calculation. Although the used methods present a deviation from another well known renowned tools, the obtained results present an accepted approximation that can be used in the conceptual stage of aircraft design.

The optimized aircraft accomplishes all objectives and respect all modeled restrictions. It is expected that after some minor modifications for latero-directional stability, the final air-frame will present a very good portability and very high endurance time.

## 12. REFERENCES

Charles A. Mader, J.R.M., 2013. "Stability-constrained aerodynamic shape optimization of flying wings". *Journal of Aircraft*.

Hepperle, M., 2005. “Airfoils for Tailless Airplanes: Design and Selection”. http://www.mh-aerotools.de/. [Online; accessed 2005].
Nickel, K. and Wohlfahrt, M., 1990. *Tailless Aircraft In Theory and Practice*. Birkhauser Verlag, Basel, 1st edition.
Simons, M., 1994. *Model Aircraft Aerodynamics*. Argus Books, England, 3rd edition.
Torenbeek, E., 2013. *Advanced Aircraft Design*. John Wiley and Sons.
Traub, L.W., 2011. “Range and endurance estimates for battery-powered aircraft”. *Journal of Aircraft*.

## 13. RESPONSIBILITY NOTICE

The authors are the only responsible for the printed material included in this paper.